International Journal of Mass Spectrometry 310 (2012) 44–51

Contents lists available at SciVerse ScienceDirect

International Journal of Mass Spectrometry

journal homepage: www.elsevier.com/locate/ijms

Metabolomic profiling for biomarker discovery in pancreatic cancer

Prabhjit Kaur[1], Kathryn Sheikh[1], Alexander Kirilyuk, Ksenia Kirilyuk, Rajbir Singh, Habtom W. Ressom, Amrita K. Cheema*

Department of Oncology, Lombardi Comprehensive Cancer Center at Georgetown University Medical Center, Washington, DC, United States

ARTICLE INFO

Article history:
Received 23 September 2011
Received in revised form 8 November 2011
Accepted 8 November 2011
Available online 18 November 2011

Keywords:
Pancreatic cancer
Metabolomics
Biomarkers
LCMS
Tissue extraction

ABSTRACT

Pancreatic cancer (PC) is the fourth leading cause of cancer death in the United States, with 4% survival, 5 years after diagnosis. Patients with pancreatic cancer are usually diagnosed at late stages, when the disease is incurable. Sensitive and more specific markers are critical for supporting new prevention, diagnostic or therapeutic strategies. Here, we report mass spectrometry-based metabolomic profiling of human pancreas matched tumor and normal tissue. Multivariate data analysis using two independent methods shows significant alterations in the profiles of the tumor metabolome as compared to the normal tissue. These findings offer an information-rich matrix for discovering novel candidate biomarkers with diagnostic or prognostic potential.

1. Introduction

Pancreas cancer (PC) is the second most frequent gastrointestinal (GI) malignancy and has a median survival of less than one year at the time of diagnosis for 96% of PC patients [1]. Pancreatic ductal adenocarcinoma (PDAC) accounts for 85–95% of pancreatic tumors [2]. A major hurdle towards improving clinical outcome of PC is the lack of diagnostic biomarkers at early stage of the disease [3]. Given the high morbidity and mortality rates associated with PC, there is an urgent need to develop specific, sensitive and cost effective biomarkers of clinical importance that can help inform treatment decisions thus improving the survival outcomes of PC patients.

Various "omics" technologies (genomics, transcriptomics, proteomics) have been used for biomarker discovery of pancreas cancer [4–7]. As the downstream complement to the other "omics", metabolomics is the comprehensive analysis of small molecule metabolites produced by normal or abnormal cellular processes. The metabolome may be considered, a more accurate representation of the cellular phenotype at any given time [8,9]. As such, it is fast gaining ground as a powerful tool to differentiate between the diseased and healthy states [10–12].

We investigated the differences in the metabolite profiles of normal and pancreas tumor tissue with a goal of developing prognostic biomarkers. For this purpose, we used ultra-performance liquid chromatography (UPLC) coupled with electrospray ionization mass spectrometry (ESI-MS) to perform small molecule metabolite profiling of matched normal and pancreatic tumor tissue. The resulting multivariate data matrix was pre-processed for spectral alignment and peak detection, followed by normalization of the data to the feature intensities of the internal standard as well as to the total protein concentration. Data mining using supervised and machine learning methods facilitated the characterization of metabolic changes in the tumor as compared to the normal tissue. We report a subset of metabolites which were unequivocally identified and were found to be significantly de-regulated in the pancreas tumor tissue type. Further characterization and validation with large sample size may help establish their utility as biomarkers of clinical benefit.

2. Materials and methods

2.1. Reagents and standards

LC/MS-grade acetonitrile (ACN), water and methanol were purchased from Fisher Scientific (NJ, USA). High purity formic acid (99%) was purchased from Thermo Scientific (Rockford, IL). MagNA Lyser green beads were purchased from Roche (Mannheim, Germany). Debrisoquine, 4-nitrobenzoic acid (4-NBA), 5′-AMP, succinate, taurine, uric acid, malic acid, uridine, glutathione, 5′-UMP, NAD, UDP-*N*-acetyl-D-glucosamine were purchased from Sigma (USA).

* Corresponding author at: Department of Oncology, Lombardi Comprehensive Cancer Center, GD9, Pre Clinical Science Building, 3900 Reservoir Road NW, Washington, DC 20057, United States. Tel.: +1 202 687 2756; fax: +1 202 687 8860.
E-mail address: akc27@georgetown.edu (A.K. Cheema).
[1] These authors contributed equally to this manuscript.

1387-3806/$ – see front matter © 2011 Elsevier B.V. All rights reserved.
doi:10.1016/j.ijms.2011.11.005

Table 1
Characteristics of patient population.

RTB#	Sex	Race	Paraffin report diagnosis
07-389	M	Not specified	Metastatic adenoid cystic carcinoma
08-461[a]	F	Caucasian	Invasive, moderately differentiated adenocarcinoma
07-298	F	Caucasian	Moderate to poorly differentiated ductal-type adenocarcinoma
07-1128	M	Caucasian	Moderately to poorly differentiated PDAC
07-1158	F	Middle Eastern	Infiltrating moderately differentiated ductal-type adenocarcinoma

[a] "Normal" tissue found to contain microtumors.

2.2. Sample collection

Five pairs of matched normal and tumor tissue samples were obtained from the Tissue and Histopathology Shared Resource repository (HTSR) of the Lombardi Comprehensive Cancer Center under board approved protocols. All samples were de-identified and assigned an alternative ID number (RTB#). The pancreatic tissue resections were acquired by HTSR, from Georgetown University Hospital under IRB approval and following guidelines specified by the NCI's Best Practices for Biospecimen Resources. Fresh pancreatic tissue was frozen in Optimal Cutting Temperature (OCT) medium immersed in a liquid nitrogen bath. Five micron sections were obtained from the tissues and stained with hematoxylin and eosin (H&E) (Supplementary Fig. S1). Pathology evaluation was performed by a board certified practicing pathologist to identify tumor and normal areas within all of the tissue blocks (Supplementary Fig. S1). The tissue samples were uniformly sectioned using a microtome (Leica CM3050 cyrostat) and processed for metabolite extraction. The clinical details are summarized in Table 1.

2.3. Metabolite extraction

For metabolite extraction, 600 μL of 50% chilled methanol containing internal standards (10 μL of debrisoquine (1 mg/mL in water) and 50 μL of 4-NBA (1 mg/mL in methanol) per 10 mL) was added to the tissue sections in MagNA Lyser tubes containing ceramic beads. The samples were homogenized using three 30 s pulses in a Magna Lyser homogenizer (Roche, USA) at 7000 rpm. The supernatant was transferred to a fresh tube and 350 μL chilled 100% ACN was added. In addition, 2 μL of the supernatant was set aside for protein quantification using the Bradford method [13]. The tubes containing supernatant and ACN were vortexed, incubated on ice for 15 min and centrifuged at 13,000 rpm at 4 °C for 15 min. The supernatant was transferred to a fresh tube and dried under vacuum. The samples were re-suspended in 200 μL of solvent A (98% water, 2% ACN) for mass spectrometry analysis.

2.4. UPLC–TOFMS profiling

Metabolites extracted from normal and tumor tissue samples were analyzed in the same batch with three technical replicates for each sample. Each sample (5 μL) was injected onto a reverse-phase 50 mm × 2.1 mm Acquity 1.7 μm C18 column (Waters Corp., Milford, MA) using an ACQUITY UPLC system online with an electrospray quadrupole time-of-flight tandem mass spectrometer (ESI-Q-TOF), as has been described [14]. The centroided data from UPLC–TOFMS acquired in the positive and negative mode was pre-processed using MarkerLynx (Waters Corp.) to generate a data matrix containing feature intensities, mass to charge (m/z) and retention time values. These data were normalized to the ion intensity of the internal standards (4-nitrobenzoic acid in the negative mode and debrisoquine in the positive mode) and total protein concentration as determined by Bradford assay.

2.5. Multivariate data analysis

The normalized data were pareto scaled [15] and analyzed first by principal component analysis (PCA) followed by orthogonal projections to latent structures (OPLS) [16] using SIMCA-P+ software (Umetrics, Kinnelon, NJ). The candidate markers were selected by examining the OPLS-S plot which is a measure of ion confidence. The ions which were distant from the point of origin in the upper right and lower left quadrant were chosen for further investigation. We also used random forest clustering [17] to interrogate the top 50 features with significant alterations in the tumor tissue as compared to the control. The candidate markers were searched against the Madison-Qingdao Metabolomic Consortium Database (MMCD) and the Human Metabolome Database (HMDB) [18,19] to find compounds that corresponded to the accurate monoisotopic mass measurements detected using UPLC–TOFMS analysis. The mass tolerance was kept at 5 parts per million to minimize false positive identifications.

2.6. Validation and targeted quantitation of metabolites

A panel of metabolites identified as having significantly altered levels in the tumor as compared to the normal tissue were validated by matching the fragmentation pattern of the parent ion to that of the standard metabolite using tandem mass spectrometry (UPLC–TOFMS/MS) and also by comparing the retention time under the same chromatographic conditions.

The quantitation was done using UPLC–TOFMS and the QuanLynx software (Waters Corp.). Briefly, all standards were analyzed in aqueous phase containing internal standards, for concentrations ranging from 10 to 50 μM in triplicates. These were used to calculate standard curves. The metabolite concentration derived from normalizing the peak intensity to that of the internal standard was then extrapolated.

3. Results and discussion

3.1. Metabolomic analysis of pancreas tissue

Metabolomic profiling of five matched pairs of normal and tumor pancreas tissue was performed using UPLC–TOFMS analysis which yielded a data matrix containing 5000 features in the positive and 2300 features in the negative mode. In order to obtain a global visualization of the metabolome for the two study groups, these data were plotted on a two dimensional scale as a function of retention time and molecular weight which yielded a peak pattern that was distinct for samples derived from normal as compared to the pancreas tumor tissue (Fig. 1). The highlighted areas in Panel A (tumor) and Panel B (normal) show differential intensity and cluster pattern of features across the mass range of 100–700 Da in a chromatographic time scale of 8.5 min. The raw data were pre-processed using the peak detection algorithm (Markerlynx, Waters Corporation) and normalized to total protein concentration to account for sampling inconsistency as well as to the ion intensities of the internal standard for error minimization resulting from run to run variation. The normalized data were analyzed using two

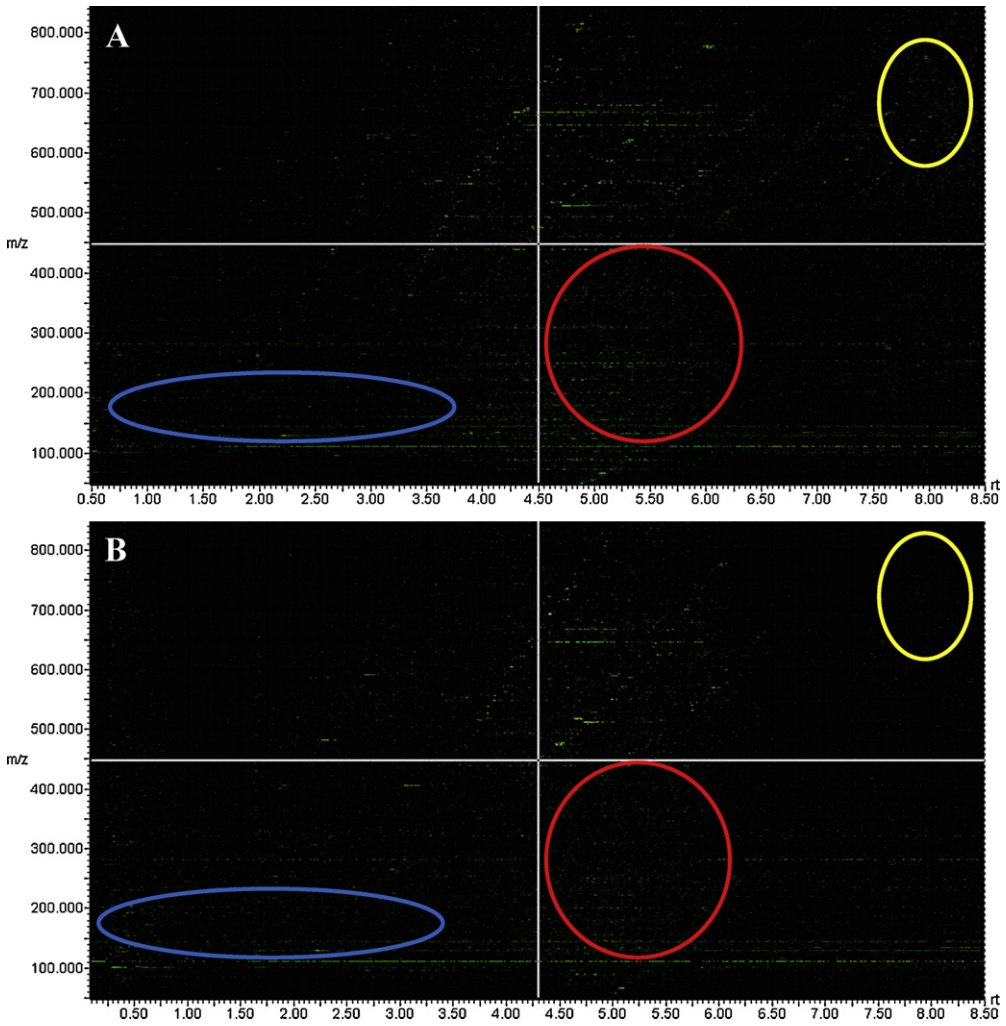

Fig. 1. Two dimensional plot of UPLC–ESI-MS data. The raw data acquired using the UPLC–ESI-MS was plotted as a function of retention time (retention time in minutes on the *X*-axis) and mass to charge ratio (*m*/*z*) of the features (in Daltons, on the *Y*-axis), to generate a two dimensional map of the distinct peak pattern in tumor (Panel A) and normal tissue extracts (Panel B). The equivalent areas in the tumor and normal samples that differed in feature pattern and intensity have been highlighted with color coded panels.

independent computational methods to decipher metabolomic differences between the pancreas tumor and normal tissue. Initially, we performed principle component analysis (PCA) using SIMCA-P+ software (Umetrics, NJ), which did not yield a clear separation of the two groups. However, OPLS analysis resulted in an unambiguous separation in the scores plot. The resulting S-plot is defined as a biomarker visualization plot of features showing significant alterations in the two groups under study which are then selected for further characterization (Fig. 2A). The mean distance from the point of origin in a S-plot, is indicative of inter-class separation. The features that are elevated in the tumor tissue are displayed in the upper right quadrant while those which are downregulated are displayed in the lower left quadrant. These candidate markers were selected for identification via mass based database search.

The data set was also analyzed using the machine learning algorithm Random forests (RF). The RF algorithm is an ensemble classifier that consists of multiple decision trees that are used to build accurate classifiers while avoiding over-fitting of the dataset. The RF was run in the R software environment. The accuracy plot for the top 50 features interrogated, resulted in a classification model with 99% accuracy (Fig. 2B) which indicates that a feature based class separation between the two groups (normal and tumor) was statistically significant. The accuracy plot shows a clear interclass separation, that is between the tumor and normal (Fig. 2B, *X*-axis) as well as a significant intra-class clustering (Fig. 2B, *Y*-axis), thus reflecting that biological replicates of each class clustered together with high degree of accuracy. The relative change for the top 50 features was plotted as a heat map (Fig. 2C), where each row represented a unique feature with a characteristic mass to charge ratio (*m*/*z*) and retention time. Interestingly, the algorithm was able to pick one outlier, which was excluded in further analysis, wherein a normal tissue sample was predicted to contain some regions of the tumor during surgical resection (Table 1).

We found a fair overlap between biomarkers found with the OPLS and Random Forest analyses which reinforced the significance of these putative markers. For instance, taurine, malic acid and UDP-*N*-acetyl-D-glucosamine in the negative mode as well as unidentified features with *m*/*z* values of 523.9791 and 287.2436 in the positive mode, were determined by both methods to be deregulated in the pancreas tumor versus normal tissue. Overall, the negative mode data set, contained more reproducible, consistent and authentic features suitable for further scrutiny as viable biomarkers of PDAC. A similar observation regarding negative mode UPLC–TOFMS metabolomics data was made by Tyburski et al. while investigating urinary metabolomic markers of radiation exposure [20].

Of the total number of significantly altered features selected from SIMCA-P+ and RF analysis, approximately twenty percent

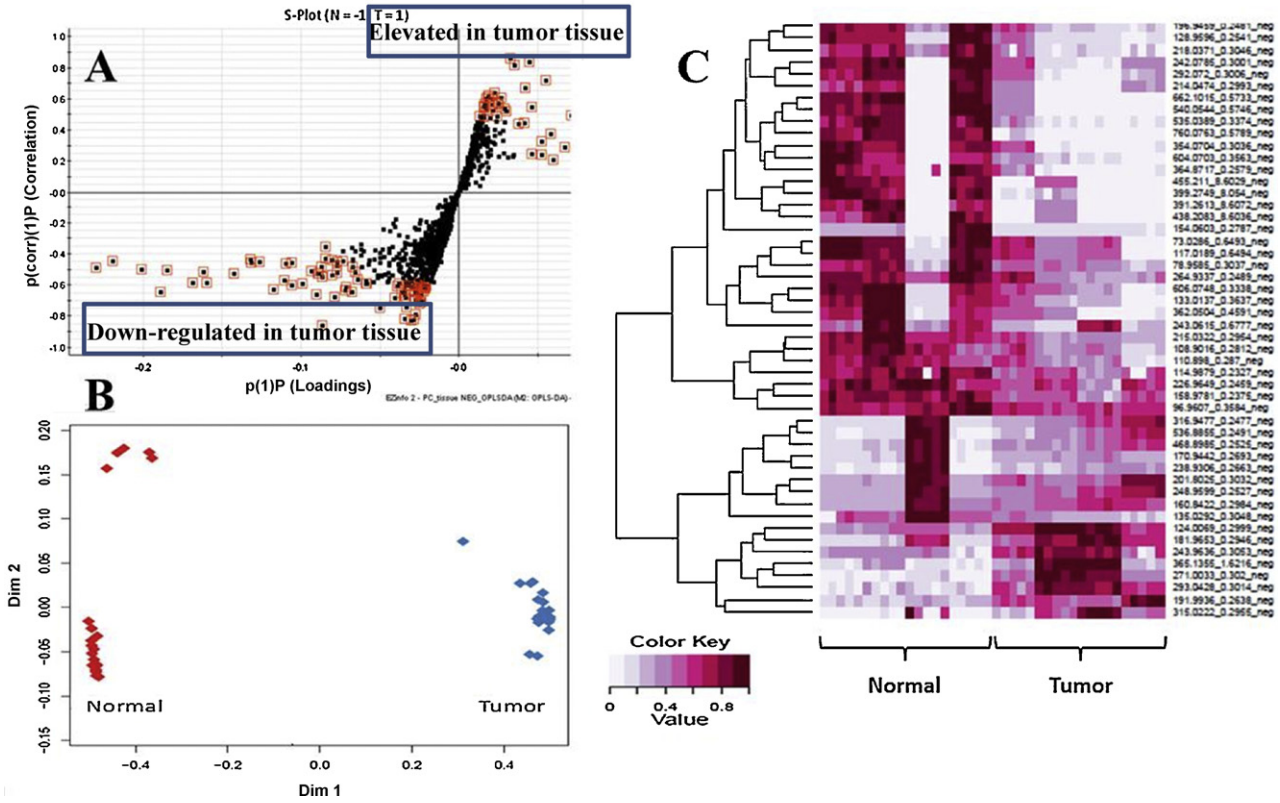

Fig. 2. Multivariate analysis of the UPLC–TOFMS data. (a) OPLS loadings S-plot comparing features from pancreatic tumor tissue extracts with those from the matched normal tissue; (b) accuracy plot for the top 50 ions interrogated using Random Forests, the first dimension depicts the interclass separation while the second dimension illustrates the intra-class separation while accuracy reflects statistical significance; (c) heat map visualization of ion rankings of top fifty features, comparing relative levels in four pairs of matched normal and pancreatic tumor tissue extracts run in quadruplicate. Each row on the heat map represents a unique feature with a characteristic mass to charge ratio and retention time value.

found a match through database search using Madison-Qingdao Metabolomic Consortium Database (MMCD) and the Human Metabolome Database (HMDB). The selected features from the analyses that were unambiguously identified with respect to their mass and retention times as well as unidentified features with a significant fold change are listed in Table 2.

3.2. Validation and relative quantitation of the candidate biomarkers

Based on the commercial availability of standard compounds, we selected a panel of fourteen candidate biomarkers for validation using tandem mass spectrometry. Authentic standards of each compound at 50 μM in 2% acetonitrile in water were used to acquire MS/MS fragmentation spectra resulting in characteristic daughter ions. The fragmentation patterns and retention times for nine features listed in Table 3, were found to be consistent between the standard and samples from the pancreatic tissue extracts. A representative fragmentation spectrum for UDP-*N*-acetyl-D-glucosamine is illustrated in Fig. 3, while the spectra for other validated markers is illustrated in Supplementary Figs. S2A–H. The major collision induced dissociation (CID) fragments as well as the TOFMS mass accuracy for each validated metabolite are listed in Table 3. These metabolites were then quantified for their relative levels, and the ratios were found to be consistent with the abundance measures predicted by the data analysis methods (Fig. 4) in the discovery mode experiments.

Table 2
Candidate biomarkers of pancreatic ductal adenocarcinoma.

Metabolite name	Kegg/PubChem ID	*m/z* (mass/charge)	RT (min)	Fold change (tumor/normal)
Succinate	C00042	117.0189 (NEG)	0.64	0.3
Taurine	C00245	124.0069 (NEG)	0.29	1.6
Malic acid	C00711	133.0137 (NEG)	0.36	0.3
Uridine	C00299	243.0615 (NEG)	0.67	0.1
Glutathione	C00051	306.0761 (NEG)	0.48	0.6
UDP-*N*-acetyl-D-glucosamine	C00043	606.0748 (NEG)	0.33	0.3
Nicotinamide adenine dinucleotide	CID 5288979	662.1015 (NEG)	0.57	0.08
5′-UMP	C01368	323.0277 (NEG)	0.37	0.4
AMP	C00020	346.055 (NEG)	0.40	0.5
Unknown	C10704	459.2029 (NEG)	5.93	3.52
Unknown	CID 6858181	523.9791 (POS)	0.29	73.1
Unknown	–	366.1397 (POS)	0.40	14.1
Unknown	C03413	287.2436 (POS)	0.36	87.9
Unknown	C00300	132.0773 (POS)	0.32	4.4
Unknown	CID 338209	188.1283 (POS)	0.39	2.0
Unknown	CID 165879	236.9944 (POS)	0.28	4.3

Table 3
Identification of significantly altered metabolites in pancreas tumor tissue using tandem mass spectrometry.

Molecule ID	Theoretical mass (Da) (−)	Observed mass (Da) (−)	ppm error	Major CID fragments
Succinate	117.0188	117.0189	0.8	99.922 73.0332
Taurine	124.0068	124.0069	0.8	106.984 79.9607
Malic acid	133.0137	133.0137	0.0	115.006 71.0174
Uridine	243.0614	243.0615	0.4	200.065 152.042 110.029
Glutathione	306.076	306.0761	0.3	272.105 128.043 143.055
UDP-*N*-acetyl-D-glucosamine	606.0737	606.0748	1.8	385.005 158.932 272.971
NAD	662.1013	662.1015	0.3	540.094 346.081 426.047
UMP	323.028	323.0277	0.9	211.017 96.974 78.9621
AMP	346.0553	346.055	0.8	134.052 96.9729 78.961

3.3. Biological significance of candidate biomarkers

Functional pathway analysis was performed by uploading the comparative metabolomics dataset into the ingenuity pathway analysis tool in order to map the metabolites to biological pathways. The network analysis revealed one major network, with enrichment of seven focus metabolites involved in the regulation of free radical scavenging, lipid metabolism and small molecule biochemistry (Fig. 5). The biological significance of interaction of metabolites like taurine and the MAPKAPK5 and the ERK1/2 signaling pathways remains to be elucidated. The functional pathway analysis showed a predominant representation of molecules involved in lipid metabolism, free radical scavenging and molecular transport (Fig. 6).

The downregulation of citric acid cycle intermediates succinate and malate may have an overall impact on the energy metabolism of the cell, while lower levels of uridine, 5′-uridine monophosphate (5′-UMP) and 5′-adenosine monophospahte (5′-AMP) could reflect rapid turnover of these nucleotides in the tumor tissue. We also observed a down-regulation of the powerful antioxidant glutathione in the pancreatic tumor tissue. A similar decrease in the serum levels of glutathione has been observed in breast carcinoma with a simultaneous increase in lipid peroxidation in plasma, which becomes more pronounced during aging of the patients [21]. There

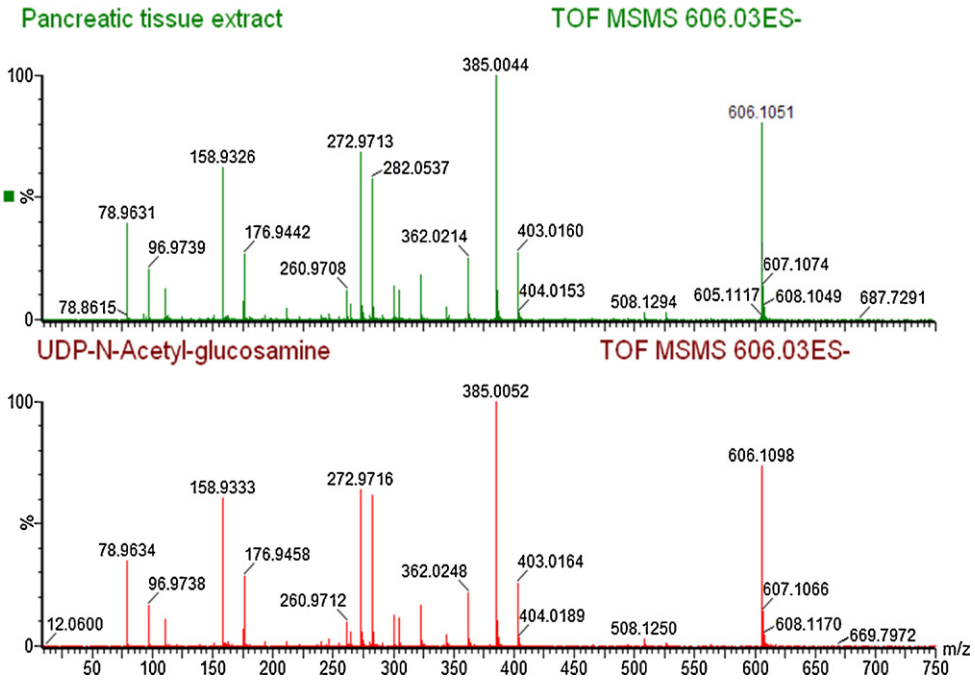

Fig. 3. Determination of the chemical structure of metabolites in pancreatic tumor tissues by tandem mass spectrometry. Top panel shows the MS/MS fragmentation of the ion with *m*/*z* 606.0748 from pancreatic tissue extracts. The bottom panel shows the fragmentation for standard UDP-*N*-acetyl-D-glucosamine.

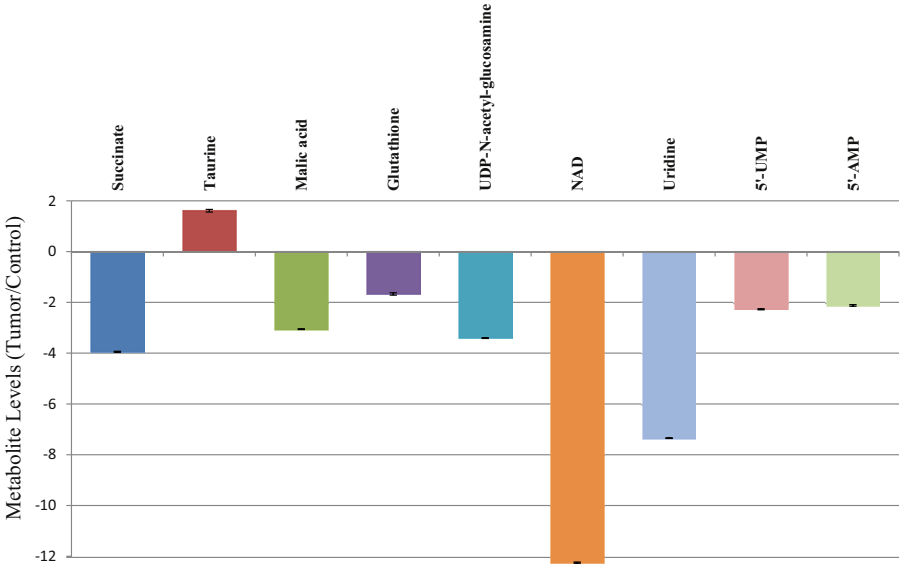

Fig. 4. Determination of relative quantitation of metabolites. Putative tissue biomarkers of pancreatic cancer were quantified by UPLC–TOFMS and QuanLynx software (see Section 2).

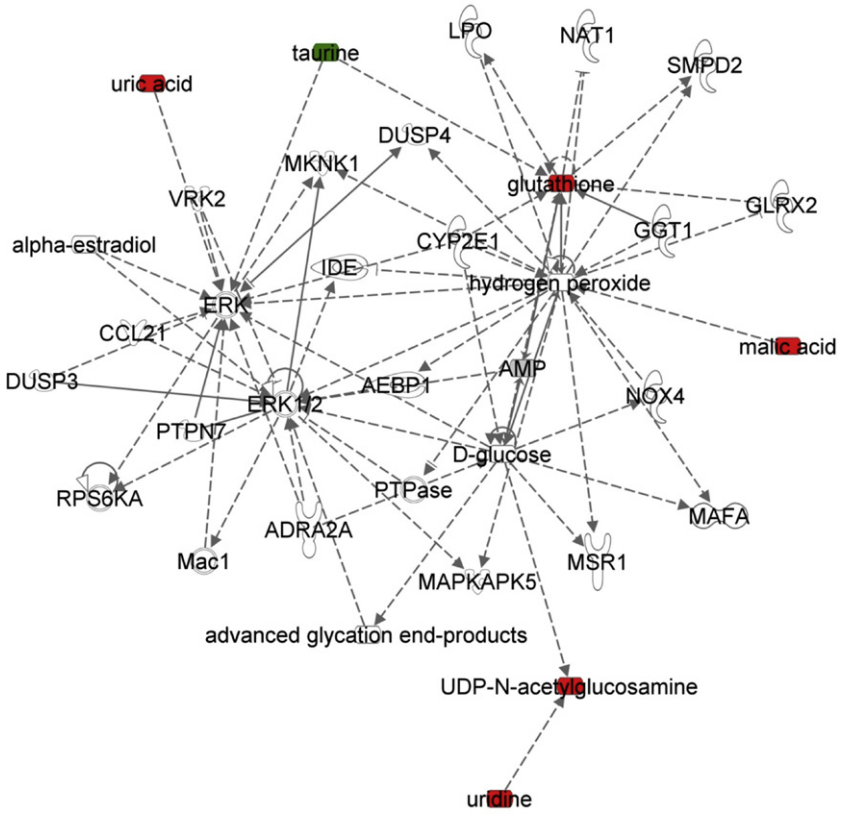

Fig. 5. Network analysis of the altered metabolites in pancreas tumor tissues. Molecular network modules for comparative metabolomics of matched pancreas tumor and normal tissue, illustrating a distinct difference in expression of participating metabolites in different cellular processes namely free radical scavenging, small molecule biochemistry and lipid metabolism. In each network module, a solid line indicates direct interaction; a dashed line indicates indirect interaction; a line without arrowhead indicates binding; an arrow from molecule A to molecule B indicates A acts on B. Node shapes are indicative: triangle, kinase; diamond, enzyme; hexagon, translation regulator; trapezoid, transporter; oval (horizontal), transcription regulator; oval (vertical), transmembrane receptor. Metabolites that are upregulated are marked in red while those that are downregulated are marked in green. In this study since the relative fold change was used as expression value type hence a greater intensity of green and red represents higher degree of down-regulation and up-regulation respectively.

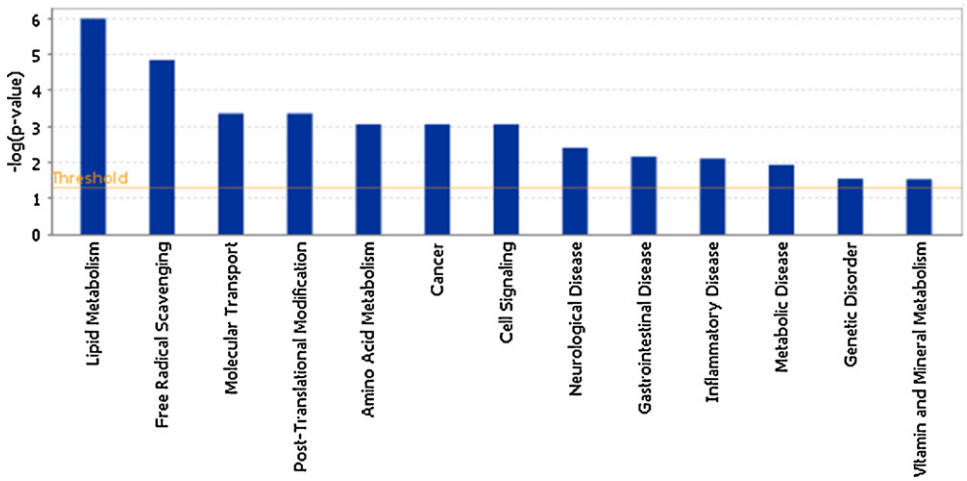

Fig. 6. Top functional pathways associated with significantly altered metabolites in pancreas tumor as compared to matched normal tissue. The ratio is calculated as the number of molecules in a given pathway that meet the cutoff criteria (0.05), divided by total number of molecules that make up that pathway. The ratio reflects the percentage of genes in a pathway that were also found in the uploaded list of significantly altered metabolites. The significance (*p*-value) looks at the association between a specific pathway and the uploaded dataset. The significance gives the confidence of association. Therefore, if a pathway has a high ratio and a very low *p*-value, the pathway is probably associated with the data and a large portion of the pathway may be involved or affected.

was an increase in the levels of amino acid taurine in the pancreatic tumor tissue as compared to the normal controls. Taurine is a major constituent of bile and has been reported to be significantly elevated in urinary bladder cancer [22]. Metabolomic profiling of plasma of pancreas cancer patients by Urayama et al. showed an elevation of taurocholic acid and tauroursodeoxycholic acid which are also constituents of bile [23].

Nicotinamide adenine dinucleotide (NAD) is an electron carrier and the NAD/NADH ratio is critical towards maintaining a redox equilibrium of a cell, a direct indicator of the metabolic health of the cell or tissue type [24]. Taken together, the alteration in the relative levels of these metabolites allow us to understand the underlying biochemical changes in pancreas tumor tissue in comparison with matched normal tissue, as well as to gain insights into the molecular basis of the progression of pancreatic carcinogenesis.

4. Conclusions

Mass spectrometry based small molecule profiling in conjunction with multivariate data analysis approaches is a powerful tool for interrogations of the tumor metabolome and complements the goals of personalized medicine. However, metabolomic profiling of samples with high complexity and biological variability presents enormous analytical challenges with respect to resolution and detection of chemically diverse small molecule metabolites and downstream analysis of the high dimensional data that is generated. In addition, unambiguous identification of metabolites presents another bottleneck in the field of LC–MS based metabolite biomarker discovery. It is expected that availability of databases with more comprehensive annotations of endogenous human metabolites will provide a strong impetus to research endeavors in this field.

Availability of reliable biomarkers for early detection of pancreas cancer as well as disease progression poses a major challenge towards improving disease outcomes. To our knowledge this is a first reported study involving UPLC–TOFMS based metabolomic profiling of pancreas tissue extracts to determine candidate biomarkers for differentiating matched tumor and normal tissue. We have also performed multivariate data analysis, metabolite identification through accurate mass based database search followed by validation using tandem mass spectrometry, relative quantitation and functional pathway analysis for the candidate biomarkers.

Our results show feasibility of such an approach for developing prognostic biomarkers with potential clinical utility. The pancreas tumor tissue offers a rich matrix for discovering biomarkers with appreciable specificity and sensitivity. We have developed a panel of candidate small molecule metabolite markers which show a significant deregulation in the pancreas tumor as compared to the matched normal tissue. Further validation using large sample cohorts is needed, to test their efficacy and performance followed by targeted validation in the body fluids to develop minimally invasive clinical assays for diagnostic and prognostic purposes.

Acknowledgements

The authors acknowledge the support of the Proteomics and Metabolomics Shared Resource and the Tissue and Histopathology Shared Resource of Lombardi Comprehensive Cancer Center NIH P30 CA5100. The authors thank Drs. Bhaskar Kallakury and Deborah Berry from HTSR for their expert advice and assistance.

Appendix A. Supplementary data

Supplementary data associated with this article can be found, in the online version, at doi:10.1016/j.ijms.2011.11.005.

References

[1] S.R. Hamilton, L.A. Aaltonen (Eds.), World Health Organization Classification of Tumors. Pathology and Genetics of Tumors of the Digestive System, IARC Press, Lyon, 2000.
[2] I. Grantzdorffer, S. Carl-McGrath, M.P. Ebert, C. Rocken, Proteomics of pancreatic cancer, Pancreas 36 (4) (2008) 329–336.
[3] R. Brand, The diagnosis of pancreatic cancer, Cancer J. 7 (4) (2001) 287–297.
[4] J.K. Stratford, D.J. Bentrem, J.M. Anderson, C. Fan, K.A. Volmar, J.S. Marron, E.D. Routh, L.S. Caskey, J.C. Samuel, C.J. Der, L.B. Thorne, B.F. Calvo, H.J. Kim, M.S. Talamonti, C.A. Iacobuzio-Donahue, M.A. Hollingsworth, C.M. Perou, J.J. Yeh, A six-gene signature predicts survival of patients with localized pancreatic ductal adenocarcinoma, PLoS Med. 7 (7) (2010) e1000307.
[5] J. Wang, J. Chen, P. Chang, A. LeBlanc, D. Li, J.L. Abbruzzesse, M.L. Frazier, A.M. Killary, S. Sen, MicroRNAs in plasma of pancreatic ductal adenocarcinoma patients as novel blood-based biomarkers of disease, Cancer Prev. Res. (Phila Pa) 2 (9) (2009) 807–813.
[6] Y. Rong, D. Jin, C. Hou, J. Hu, W. Wu, X. Ni, D. Wang, W. Lou, Proteomics analysis of serum protein profiling in pancreatic cancer patients by DIGE: up-regulation of mannose-binding lectin 2 and myosin light chain kinase 2, BMC Gastroenterol. 10 (2010) 68.

[7] S. Tonack, M. Aspinall-O'Dea, J.P. Neoptolemos, E. Costello, Pancreatic cancer: proteomic approaches to a challenging disease, Pancreatology 9 (5) (2009) 567–576.
[8] N. Blow, Metabolomics: biochemistry's new look, Nature 455 (7213) (2008) 697–700.
[9] J.K. Nicholson, J.C. Lindon, Systems biology: metabonomics, Nature 455 (7216) (2008) 1054–1056.
[10] T.F. Bathen, L.R. Jensen, B. Sitter, H.E. Fjosne, J. Halgunset, D.E. Axelson, I.S. Gribbestad, S. Lundgren, MR-determined metabolic phenotype of breast cancer in prediction of lymphatic spread, grade, and hormone status, Breast Cancer Res. Treat. 104 (2) (2007) 181–189.
[11] A. Sreekumar, L.M. Poisson, T.M. Rajendiran, A.P. Khan, Q. Cao, J. Yu, B. Laxman, R. Mehra, R.J. Lonigro, Y. Li, M.K. Nyati, A. Ahsan, S. Kalyana-Sundaram, B. Han, X. Cao, J. Byun, G.S. Omenn, D. Ghosh, S. Pennathur, D.C. Alexander, A. Berger, J.R. Shuster, J.T. Wei, S. Varambally, C. Beecher, A.M. Chinnaiyan, Metabolomic profiles delineate potential role for sarcosine in prostate cancer progression, Nature 457 (7231) (2009) 910–914.
[12] F. Sullentrop, D. Moka, S. Neubauer, G. Haupt, U. Engelmann, J. Hahn, H. Schicha, 31P NMR spectroscopy of blood plasma: determination and quantification of phospholipid classes in patients with renal cell carcinoma, NMR Biomed. 15 (1) (2002) 60–68.
[13] B.J. Olson, J. Markwell, Assays for determination of protein concentration, Curr. Protoc. Pharmacol., 2007, Appendix 3, 3A.
[14] R.S. Varghese, A. Cheema, P. Cheema, M. Bourbeau, L. Tuli, B. Zhou, M. Jung, A. Dritschilo, H.W. Ressom, Analysis of LC–MS data for characterizing the metabolic changes in response to radiation, J. Proteome Res. 9 (5) (2010) 2786–2793.
[15] I. Noda, Scaling techniques to enhance two-dimensional correlation spectra, J. Mol. Struct. 883–884 (2008) 216–227.
[16] J.W.S. Trygg, Orthogonal projections to latent structures (O-PLS), J. Chemom. 16 (2002) 119–128.
[17] L. Breiman, Random forests, Mach. Learn. 45 (2001) 5–32.
[18] Q. Cui, I.A. Lewis, A.D. Hegeman, M.E. Anderson, J. Li, C.F. Schulte, W.M. Westler, H.R. Eghbalnia, M.R. Sussman, J.L. Markley, Metabolite identification via the Madison Metabolomics Consortium Database, Nat. Biotechnol. 26 (2) (2008) 162–164.
[19] D.S. Wishart, C. Knox, A.C. Guo, R. Eisner, N. Young, B. Gautam, D.D. Hau, N. Psychogios, E. Dong, S. Bouatra, R. Mandal, I. Sinelnikov, J. Xia, L. Jia, J.A. Cruz, E. Lim, C.A. Sobsey, S. Shrivastava, P. Huang, P. Liu, L. Fang, J. Peng, R. Fradette, D. Cheng, D. Tzur, M. Clements, A. Lewis, A. De Souza, A. Zuniga, M. Dawe, Y. Xiong, D. Clive, R. Greiner, A. Nazyrova, R. Shaykhutdinov, L. Li, H.J. Vogel, I. Forsythe, HMDB: a knowledgebase for the human metabolome, Nucleic Acids Res. 37 (2009) D603–D610 (Database issue).
[20] J.B. Tyburski, A.D. Patterson, K.W. Krausz, J. Slavik, A.J. Fornace Jr., F.J. Gonzalez, J.R. Idle, Radiation metabolomics. 2. Dose- and time-dependent urinary excretion of deaminated purines and pyrimidines after sublethal gamma-radiation exposure in mice, Radiat. Res. 172 (1) (2009) 42–57.
[21] J. Kasapovic, S. Pejic, V. Stojiljkovic, A. Todorovic, L. Radosevic-Jelic, Z.S. Saicic, S.B. Pajovic, Antioxidant status and lipid peroxidation in the blood of breast cancer patients of different ages after chemotherapy with 5-fluorouracil, doxorubicin and cyclophosphamide, Clin. Biochem. 43 (2010) 1287–1293.
[22] S. Srivastava, R. Roy, S. Singh, P. Kumar, D. Dalela, S.N. Sankhwar, A. Goel, A.A. Sonkar, Taurine—a possible fingerprint biomarker in non-muscle invasive bladder cancer: a pilot study by 1H NMR spectroscopy, Cancer Biomark. 6 (1) (2010) 11–20.
[23] S. Urayama, W. Zou, K. Brooks, V. Tolstikov, Comprehensive mass spectrometry based metabolic profiling of blood plasma reveals potent discriminatory classifiers of pancreatic cancer, Rapid Commun. Mass Spectrom. 24 (5) (2010) 613–620.
[24] D.H. Williamson, P. Lund, H.A. Krebs, The redox state of free nicotinamide-adenine dinucleotide in the cytoplasm and mitochondria of rat liver, Biochem. J. 103 (2) (1967) 514–527.